Submitted for publication in the IEEE Trans. on Nuclear Science, December 1993 issue.

ON-CHIP p-MOSFET DOSIMETRY

M. G. Buehler, B. R. Blaes, G. A. SoIi, and G. R. Tardio
Jet Propulsion Laboratory 300-329
4800 Oak Grove Drive
Pasadena, CA91109

ABSTRACT

On-chip p-FETs were developed to monitor the radiation dose of n-well CMOS ICs by monitoring the threshold voltage shifts due to radiation induced oxide and interface charge. The design employs closed geometry FETs and a zero-biased n-well to eliminate leakage currents. The FETs are operated using a constant current to greatly reduce the FET's temperature sensitivity. The dose sensitivity of these p-FETs is about -2.54 mV/krad(Si) and the off-chip instrumentation resolves about 400 rads/bit. When operated with a current at the temperature-independent point, the output voltage, VO, is located near 1.5 V and depends on VT, VT_T, and n. VTT is typically 2 mV/°C but, with temperature compensation, VOT is less than 30 µV/°C over a 70"C temperature span.

INTRODUCTION:

The use of FETs (Field-Effect Transistors) as dosimeters was pioneered by Holmes-Siedle [1]. A number of these devices have flown on earth bound satellites [2 - 4].

In recent years p-FETs dosimeters have been developed with specially grown gate oxides which have a large number of oxide traps and sensitivities of <1 mV/rad(Si) [5] have been achieved. The sensitivity to radiation can also be enhanced by applying a large negative bias during radiation which forces more of the oxide charge to the interface. The need to operate the p-FETs with a current at the temperature-independent point has been recognized [6, 7].

In the following effort, a p-FET dosimeter is developed under the constraint that the dosimeter be useful in predicting the radiation dose of an IC fabricated with a non-radiation hardened CMOS process. As shown in Fig. 1, two p-FETs are included on the RADMON, Radiation Monitor, which also includes an SEU-SRAM for monitoring particle upsets. The RADMON was designed for use on the STRV (Space Technology Research Vehicle) to be launched in 1994.

The p-FET uses available CMOS biases during measurement and is unbiased when not being measured. This approach to biasing is intended to provide a known bias environment. In certain applications, the availability of spacecraft power is unpredictable. Thus being unpowered, during dosing, provides a known bias environment.

On-chip dosimetry provides the advantage that the dose is measured directly. This reduces the uncertainty inherent in dosimetry calculations which are complicated especially for highly embedded electronics.

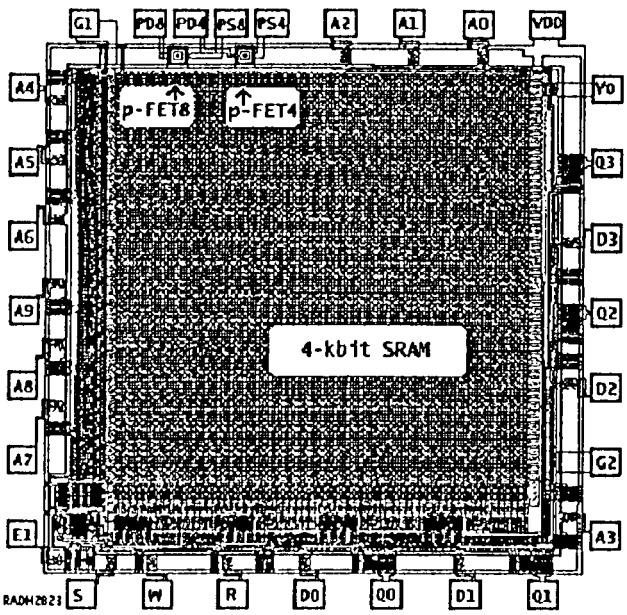

Figure 1. STRV-RADMON Chip 1.6 mm x 1.7 mm.

P-FET DESIGN

The layout of the p-FET, shown in Fig. 2, and features a closed geometry design where the drain is completely surrounded by the source. The cross section of the device, shown in Fig. 3, indicates that the n-well and source are separated so that they can operate at slightly different biases. In addition the n-well is grounded. In a CMOS circuit the n-

well is normally connected to VDD. These design precautions minimize leakage currents.

COMPLETE p-FET MODEL EQUATIONS

As seen in Fig. 3, the gate is connected to the drain. This ensures that the p-FET is operated in the saturation region. In saturation the drain current is given by [7]:

$$(1)\quad ID = \frac{\beta}{2}\cdot\frac{(VO - VT)^2}{1 + \theta(VO - VT)}$$

where VO is the p-FET output voltage, $\beta = KP\cdot W/L$, $KP = \mu_0\cdot C$ and VT is the absolute value of the p-FE? threshold voltage. The other parameters are We and L_e are the effective channel width and length respectively. μ_0 is the zero-field channel mobility, Co is the gate oxide capacitance per unit area, and θ is the mobility electric-field degradation parameter.

This equation is plotted in Fig. 4 which shows that the "temperature independent" point is in fact ill-defined when viewed in detail .

The above parabolic equation was linearized by taking the square root and then applying the Taylor Series expansion to the θ term:

$$(2)\quad \sqrt{ID} = \sqrt{\beta/2}(VO - VT)\left[1 - \frac{\theta}{2}(VO-VT)\right]$$

The temperature and dose dependence of VT, 13, and θ are given below. For the threshold voltage:

$$(3)\quad VT = VT_0 + VT_T(T - To) + VT_D\cdot D$$

where To is the the reference temperature taken as 300 K, $VTT = \partial VT/\partial T|_{T\to To}$ and $VTD = \partial VT/\partial D|_{D\to 0}$. The temperature and dose dependence of β is given by:

$$(4)\quad \beta = \beta_0(T/T_0)^{-n} + \beta_D\cdot D$$

where $\beta_D = \partial\beta/\partial D|_{D\to 0}$ n characterizes the mobility temperature dependence, and T is the absolute temperature. Note that:

$$(5)\quad \beta_T = \partial\beta/\partial T = -n\cdot\beta/T$$

The temperature and dose dependence of θ is given by:

$$(6)\quad \theta = \theta_0 + \theta_T\cdot(T - T_0) + \theta_D\cdot D$$

where $\theta_T = \partial\theta/\partial T|_{T\to To}$ and $\theta_D = \partial\theta/\partial D|_{D\to 0}$.

The p-FET output voltage follows from Eq. 2 after solving tbe quadratic equation in VO:

$$(7)\quad VO = VT + \frac{1}{\theta}\cdot(1 - \sqrt{1 - \theta\cdot\sqrt{[8\cdot ID/\beta]}})$$

where the sign of the square root sign is negative which can be seen in the limit where $\theta = 0$. Next ID_m is found from the above equation by setting $\partial VO/\partial T = 0$ and solving the resulting quadratic equation for ID_m:

$$(8)\quad \sqrt{ID_m} = -\frac{A}{2} - C \pm D\sqrt{[1 + B\cdot(C + A/4)]}$$

The sign of the square root is positive for $\theta > 0$ and negative for $\theta < 0$. The primary parameters are:

(9) A=a2b/d2
(10) B = b
(11) C = c/d
(12) D= a/d

and the secondary parameters are:

(13) a = $\sqrt{VTT} - \sigma_T/\theta_m^2$
(14) b = $\theta_m\cdot\sqrt{(8/\beta_m)}$
(15) c = $-\theta_T/\theta_m^2$
(16) d= $[(2\theta_T/\theta_m) - (n/T_m)]/\sqrt{(2\beta_m)}$

Once ID_m is calculated using the above algorithm, VD_m is calculated using Eq 5.25 evaluated at T_m:

$$(17)\quad VO_m = VT_m + \frac{1}{\theta_m}\cdot(1 - \sqrt{1 - \theta_m\cdot\sqrt{(8ID_m/\beta_m)}})$$

SIMPLIFIED p-FET MODEL EQUATIONS (θ = 0)

Physical insight results by deriving the model equations for $\theta = 0$. From Eq. 2 the output voltage is:

$$(18)\quad VO = VT + \sqrt{2ID/\beta}$$

The temperature sensitivity of VO is calculated using Eqs. 3 and 4 for D = 0. The result is plotted in Fig. 5. If the current is chosen correctly, the operating temperature span is more than 70°C for less than 1 mV change in VO. This translates in to a temperature sensitivity for VO of less than 30 μV/°C. If the uncertainty in the current is ±1 percent, the operating span is reduced to 60"C for less than a 1 mV change in VO. In general the current must be chosen within 1 percent of the target current.

The current at the temperature independent point for θ = 0 follows by setting the temperature differential of Eq. 18 to zero:

$$(19)\quad ID_m = 2\beta_m^3(VT_T/\beta_{Tm})^2$$

Substituting $\beta_m = KP_mW/L$ and Eq. 5 leads to:

(20) $ID_m = 2KP_m(VT_T \cdot T_m/n)^2 W/L$

This shows that ID_m depends on the FET geometry and the silicon parameters. Thus once the silicon parameters are known, ID_m is known given T_m and W/L.

The output voltage at the temperature independent point is found by substituting Eqs. 5 and 19 into Eq. 18:

(21) $VO_m = VT_m - 2VT_T \cdot T_m/n$

which shows that VO_m is independent of the FET W/L geometry and depends only on the silicon parameters. Values for VO_m range between 1.5 and 2 V for modern p-FET devices.

It is of technological interest to note that VO_m is independent of temperature for n = 2. This means that a true temperature independent point can be achieved. Combining Eqs. 4, 5, 18, and 19 leads to:

(22) $VOT = \partial VO/\partial T = VT_T[1 - (Tin/T)^{1-n/2}]$

This shows that $VO_T = 0$ at $T = T_m$ for any n and VOT = 0 for n = 2 for all T.

p-FET TEMPERATURE DATA ANALYSIS

The p-FETs were measured in packages using an hp4062 parametric test system with an oven. The measurements were obtained by forcing VO = 3 V and measuring ID_5. Then four additional currents were forced at $\sqrt{ID_1} = 0.2 \cdot \sqrt{ID_5}$, $\sqrt{ID_2} = 0.401/I_5$, $\sqrt{ID_3} = 0.6 \cdot \sqrt{ID_5}$, and $\sqrt{ID_4} = 0.8 \cdot \sqrt{ID_5}$. These IV points were fitted using Eq. 23. The B, VT, and θ values are listed in Table 1 for three temperatures estimated to be accurate within 1°C.

The experimental data, shown in Fig. 6, was fitted using the method of least squares. In the analysis the following parabolic equation was fitted to the data and then the coefficients were related to the parameters in Eq. 2.

(23) $\sqrt{ID} = a_0 + a_1 \cdot VO + a_2 \cdot VO^2$

where

(24) $a_0 = -\sqrt{(B/2)} \cdot VT \cdot (1+\theta \cdot VT/2)$

(25) $a_1 = \sqrt{(B/2)} \cdot (1+\theta \cdot VT)$

(26) $a_2 = -\sqrt{(B/2)} \cdot \theta/2.$

The parameters a_0, a_1, and a2 are used to obtain the FET parameters for each of the IV curves. The solution for VT was obtained by recognizing that VO = VT at ID = 0. This leads to a quadratic equation whose solution is:

(27) $VT = a_1/(2a_2) \cdot (-1+\sqrt{1-4a_0a_2/a_1^2})$

The sign of the square root is positive for positive VT values. Next the solution for B was found by recognizing that at VO = VT, $\partial\sqrt{ID}/\partial VO|_{VO=VT} = \sqrt{(B/2)} = 2a_2 \cdot VT + a_1$; thus

(28) $B = 2(2a_2 \cdot VT + a_1)^2$

Finally, θ follows by recognizing that the parameter $a2 = -(\theta/2) \cdot \sqrt{(B/2)}$; thus

(29) $\theta = -1/[VT + a_1/(2a_2)]$

The temperature parameters for VT and θ were extracted by least squares fitting the data using Eqs. 3 and 6. The temperature parameter for B was extracted from Eq. 4 after it was linearized by taking the logarithm. The temperature parameters are listed in Table 2.

p-FET DOSE DATA ANALYSIS

The p-FET dose dependence was determined using Cobalt-60 irradiation. The devices were-irradiated with their lids on, at room temperature, at 40 rads/see, and at zero bias. The p-FETs were measured within 15 minutes after Cobalt-60 irradiation.

The p-FET irradiation results, shown in Fig. 7, were least squares fitted using the algorithm given in Eq. 23. This produced a set of VT, B, and θ values for each dose value. These are plotted in Figs. 8 to 10 for four p-FETs. The radiation results are listed in Table 3.

The VT values, plotted in Fig. 8, show some nonlinearity with dose because of the high dose rate of 40 rads/sec. The VT anneals after one-week, as shown at the highest dose value. Using this value, the slope of the VT vs dose curve is VTD = -1.56 mV/krad(Si). These results are explained by the build-up of positive oxide and interface charge and loss of oxide charge during anneal.

The B values, shown in Fig. 9, are separated by the difference in the W/L ratios between the p-FETs. The B continues to shift after an 18 hr anneal shown at 120 in Fig. 10. These results are explained by the build up of positively charged interface states during irradiation and anneal and this affects the zero-field hole channel mobiity.

The θ values are shown in Fig. 10. These curves are clustered about the W/L ratio and

they continue to shift after an 18 hr anneal shown at 120 in Fig. 10. Notice that θ is positive initially and negative after irradiation and anneal.

As far as the author's know, the field-dependent mobility after dosing was discussed only once before in the literature [8]. The positive and negative θ values are explained by the mobility values shown in Fig. 11. These values were calculated from:

$$(30)\quad \mu = 2L \cdot ID/[W \cdot C_o \cdot (VO - VT)^2]$$

where Co was calculated for a 21.8 nm oxide. As seen in Fig 11, for D = O, the mobility decreases as the field increases. After radiation, the mobility is degraded at zero-field and this explains the decrease in β with dose. But after a heavy dose the mobility increases with field. This is explained by the channel charge shielding the interface states and preventing the interface states from acting as scattering centers.

5.10 DOSIMETRY

The damage factor for the dose calculations is derived in this section. Since the dose is measured at the constant current, ID_m, the radiation dose sensitivity of VO is greater than VTD. This is evident in Fig. 8 where the spread in the curves is wider at ID = ID_m than at ID = O due to β's dose dependence.

In this section the damage factor, VOD, for θ = O is calculated by differentiating Eq. 5.10 with respect to dose. Then the constant current ID_m given in Eq. 19 is substituted in to the result. The damage factor is:

$$(31)\quad VO_{Dm} = \partial V/\partial D = VTD - VTT \cdot \beta_{Dm}/\beta_{Tm}$$

Results for a p-FET were calculated using VTD = -1.86 mV/krad(Si), KP_{Dm} = -0.053 $(\mu A/V^2)$/krad (Si), VTT = +1.80 mV/°C, and KP_{T_M} = -0.14 $(\mu A/V^2)$/°C. This leads to a damage factor of VO_{Dm} = -2.54 mV/krad(Si).

CONCLUSION

The use of on-chip p-FET dosimeters is quite feasible an provides good sensitivity if the FETs are operated at the temperature independent point. The use of on-chip p-FETs provides a direct measure of the worst case radiation dose experienced by the associated CMOS IC.

REFERENCES:

1. A. Holmes-Siedle, "The space-charge dosimeter - General principles of a new method of radiation detection," Nucl.Instr. & Methods, Vol. 121, 169-179 (1974).

2. E. G. Stassinopoulos, et. al., "Prediction and measurement results of radiation damage to CMOS devices on board spacecraft," IEEE Trans. Nucl. Sci., NS-24, 2289-2293 (1977).

3. A. Holmes-Siedle, et. al., "Calibration and flight testing of a low-field pMOS dosimeter," IEEE Trans. Nucl. Sci., NS-32, 4425-4429 (1992).

4. G. A. Soli, et. "al., "CRRES microelectronic test chip orbital data 11," IEEE Trans. Nucl. Sci., NS-39, 1840-1845 (1992).

5. A. Holmes-Siedle, et. al., "MOS dosimeters - Improvement of responsivity," RADECS91, 65-69 (1991).

6. M. O'Sullivan, et. al., "Temperature compensation of PMOS dosimeters," Proc. ESA Electronics Components Conf, ESTEC, 281-285 (November 1990).

7. Y. P. Tsividis, Operation and Modeling of the MOS Transistor, McGraw-Hill (New York, 1987).

8. K. A. Ports, "A process for the simultaneous production of radiation hardeded complementary linear bipolar and linear metal gate CMOS devices," IEEE Trans. Nucl. Sci., NS-27, 1721-1726 (1980).

ACKNOWLEDGMENT:

The research described herein was performed by the Center for Space Microelectronics Technology, Jet Propulsion Laboratory, California Institute of Technology, and was sponsored by the Strategic Defense Initiative Organization. The authors are indebted to MOSIS for brokering the CMOS fabrication.
File: NSRE3620.DOC

Table 1. Flight p-FET4 parameters (W12P4C26)

T °C	|VT| V	β mA/V²	θ l/v
30	0.874	1.100	0.056
75	0.800	0.891	0.041
125	0.703	0.708	0.027

Table 2. Flight p-FET Parameters
(T_o = 20°C, T_m = 10"C, W12P4C26)

PARAM	UNITS	MEAN STDEV
W	urn	182
L	urn	4
VT_o	V	-0.8944±0.0055
VTT	mV/°C	1.8002*0.0800
B_o	mA/V^2	1.1667±0.0126
KP_o	$\mu A/V^2$	25.6421?0.2774
n	--	1.6139*0.0528
θ_o	1/v	0.0593±0.0014
θ_T	1/(kV·°C)	-0.3153*0.0209
VT_m	v	-0.9125
B_m	mA/V^2	1.2339
θ_m	1/V	0.0624
ID_m	μA	244
VO_m	V	-1.55

Table 3. Ground Test p-FET Cobalt-60 Radiation Parameters W12P4C28

PAR.	UNITS	MEAN STDEV
VTD	mV/krad(Si)	-1.85620.097
B_D	PA/V^2/krad(Si)	-2.401±0.048
KP_D	$\mu A/V^2$/krad (Si)	-0.053±0.001
θ_D	1/kV/krad(Si)	-0.841*0.026

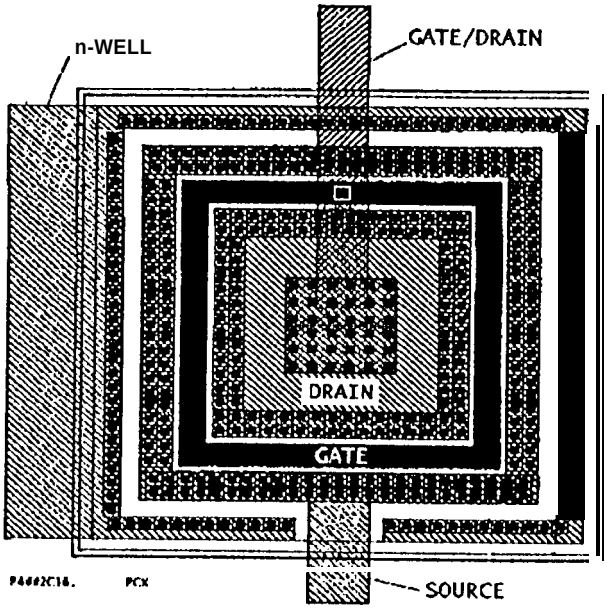

Figure 2. p-FET, MP4, layout where L = 4 μm and W = 182 μm. (File: P4##2C16.PCX)

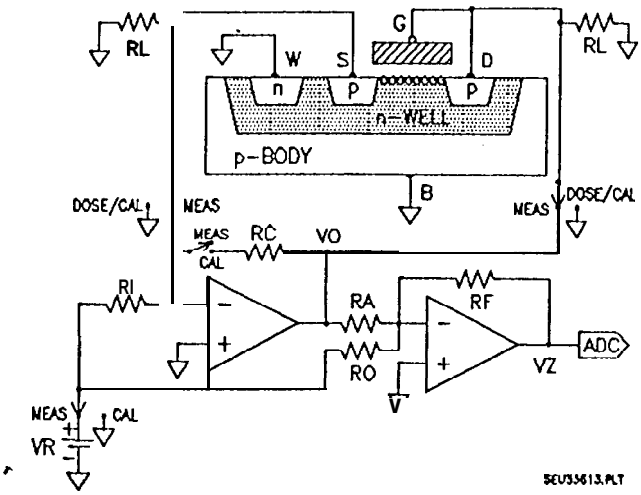

Figure 3. p-FET total dose circuitry.

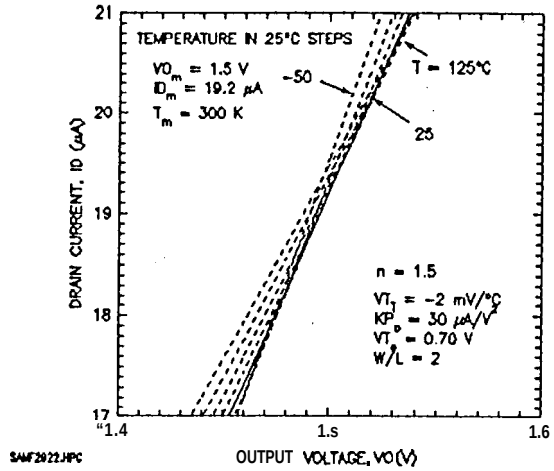

Figure 4. Expanded p-FET IV characteristics showing that the "temperature independent" point is not a point.

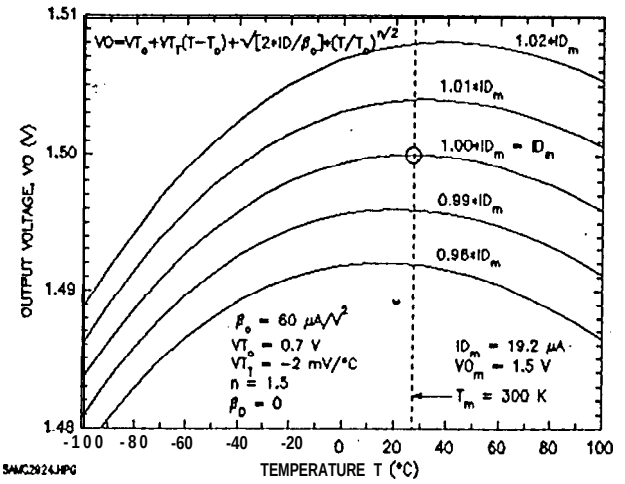

Figure 5. The temperature and current dependence of the p-FET output voltage.

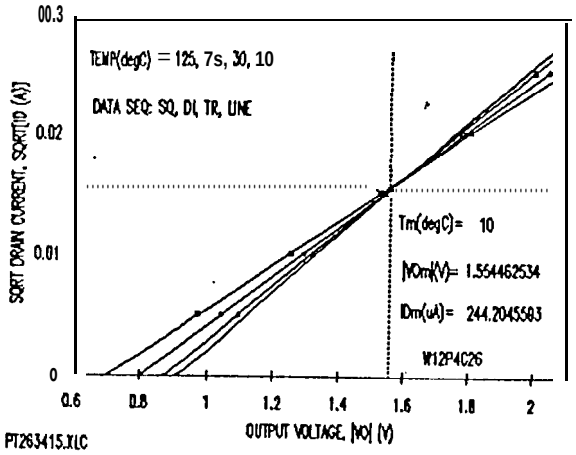

Figure 6. Temperature dependence of flight p-FET W12P4C26.

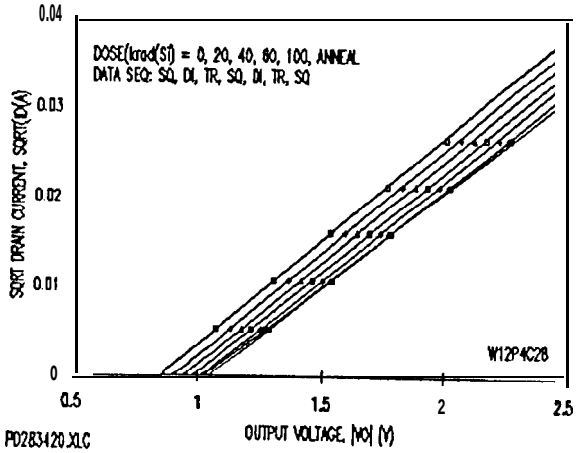

Figure 7. p-FET Cobalt-60 dose/anneal dependence where the point at 120 was measured 18 hr after last dose.

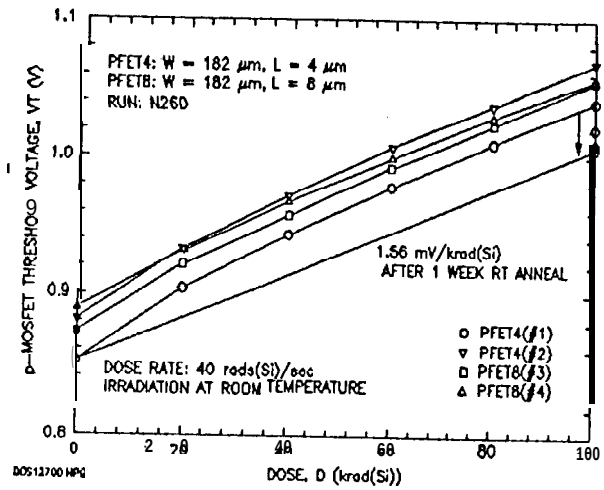

Figure 8. 1.2-µm CMOS p-FET total dose response after one-week anneal.

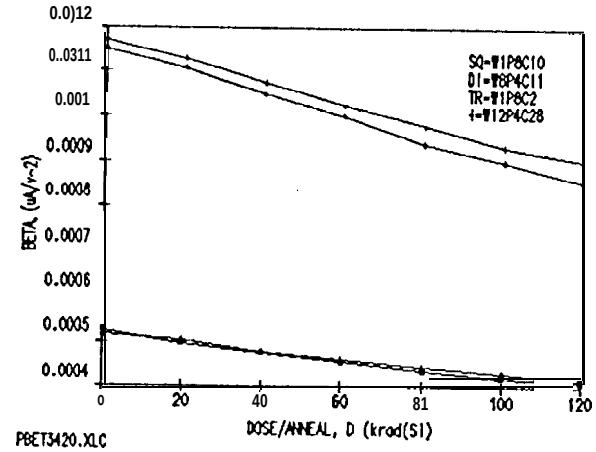

Figure 9. 1.2-µm CMOS p-FET beta Cobalt-60 dose/anneal dependence.

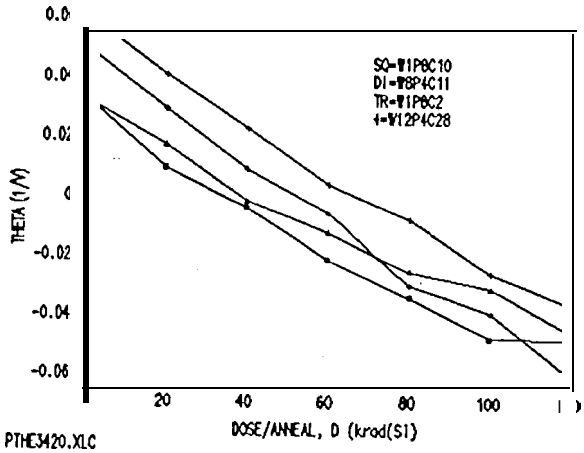

Figure 10. 1.2-µm CMOS p-FET theta Cobalt-60 dose/anneal dependence.

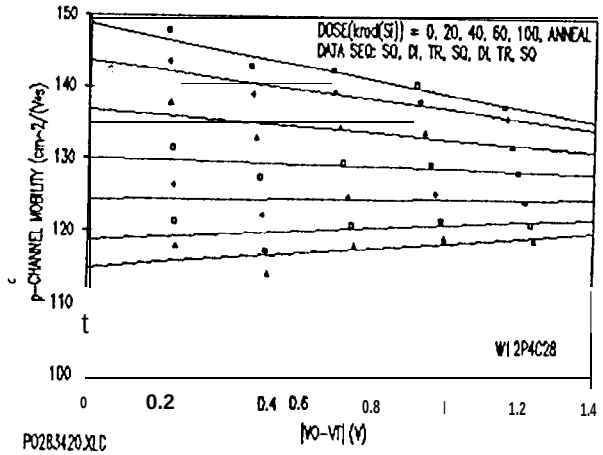

Figure 11. 1.2-pm CMOS p-FET channel mobility after Cobalt-60 dose and anneal. Chip No. W12P4C28.